

VISCOSITY AND ION-NEUTRAL EFFECTS ON PLASMA ROTATION IN STELLARATORS

J.N. TALMADGE, B.J. PETERSON, D.T. ANDERSON,
F.S.B. ANDERSON, H. DAHI, J.L. SHOHET
Torsatron/Stellarator Laboratory,
University of Wisconsin,
Madison, Wisconsin,
United States of America

M. CORONADO
Instituto de Ciencias Nucleares,
Universidad Nacional Autónoma de México,
Mexico

K.C. SHAINING
Oak Ridge National Laboratory,
Oak Ridge, Tennessee,
United States of America

M. YOKOYAMA, M. WAKATANI
Plasma Physics Laboratory,
Kyoto University,
Uji, Kyoto,
Japan

Abstract

VISCOSITY AND ION-NEUTRAL EFFECTS ON PLASMA ROTATION IN STELLARATORS.

Measurements of the radial electric field, flow velocity and momentum decay times were made in the IMS stellarator as a function of neutral pressure, during biased electrode experiments, to determine the relative importance of viscosity and ion-neutral collisions to momentum damping. The radial electric conductivity and plasma flows are dominated by collisions with neutrals in the interior of the plasma and by viscosity at the edge in approximate agreement with a neoclassical model. The theory of L-H transition in tokamaks is extended to stellarators. In a stellarator geometry, the poloidal viscosity can have multiple local maxima at a poloidal Mach number $M_p \sim |m - nq|/m$, where $m(n)$ is the poloidal (toroidal) mode number and q is the safety factor. If the neutral density is too high, the local maxima in the viscosity disappear and no L-H transition will occur.

1. INTRODUCTION

The relative contribution of plasma viscosity and ion-neutral collisions to momentum damping in a tokamak or stellarator may be an important factor in determining the radial electric conductivity and plasma flows, especially near the plasma edge in large devices where the neutral density is non-negligible. In the Interchangeable Module Stellarator (IMS), the molecular hydrogen profile is roughly uniform for low-density ($0.5\text{--}2.0 \times 10^{11} \text{ cm}^{-3}$), weakly-ionized ECH discharges. The mean free path for molecular hydrogen is approximately 2 m, much greater than the plasma minor radius ($\bar{a} \approx 4.5 \text{ cm}$). On the other hand, the magnetic field ripple, and hence the plasma viscosity, increase strongly with minor radius. In the Pfirsch-Schlüter collisionality regime the viscosity is inversely proportional to the ion collision frequency, which includes collisions with neutrals if the neutral density is sufficiently large. In contrast, the damping due to ion-neutral collisions alone is proportional to the ion-neutral collision frequency. The relative importance of viscosity and ion-neutral collisions to momentum damping is studied in IMS by varying the neutral pressure and measuring the resulting change in the radial electric conductivity, flow velocity and ion flow damping time at two radial locations in the plasma where the viscosity differs appreciably.

The relative damping due to viscosity and collisions with neutrals may also be an important factor in achieving an L-H transition. A mechanism that can explain the L-H transition in tokamaks is based on the bifurcation of the radial electric field E_r through the existence of a local maximum in the plasma viscosity and the subsequent suppression of the turbulence fluctuations due to the shear of the $E \times B$ flow [1-3]. Plasma viscosity has a local maximum located at a critical poloidal $E \times B$ Mach number $M_p = (V_E B / v_t B_p)$ of the order of unity, as shown in CCT [4] and TEXTOR [5] and can also be inferred from the JFT-2M [6] and DIII-D [7] data. Here, V_E is the poloidal $E \times B$ drift speed, v_t is the ion thermal speed, and B_p is the poloidal magnetic field strength. The theory of L-H transitions in tokamaks is extended to stellarators by considering both the toroidal and helical components to the magnetic field spectrum. Also, the effect of charge-exchange momentum loss on the transition is discussed.

In this paper, ion-neutral collisions and plasma viscosity are considered at two regimes of the plasma flow velocity. In Sec. 2 the viscosity is linearly dependent on the flow velocity at small rotation speeds. In Sec. 3, where L-H transitions are considered, the viscosity is nonlinear at large flow speeds.

2. RADIAL ELECTRIC FIELD AND ION FLOWS IN IMS

From Ref. [8], the steady-state solutions to the continuity and momentum balance equations yield an expression for the radial conductivity in the form $\langle J \cdot \nabla V \rangle = \sigma_r [E \cdot \nabla V - 1/eN\nabla p \cdot \nabla V]$ where σ_r is the plasma radial conductivity given by

$$\sigma_r = \frac{c^2 MN}{(\nu_\theta + \nu_\zeta + \nu_{in})} \frac{1+2q^2}{B_0^2} \left[(\nu_\theta^P + \nu_{in})(\nu_\zeta + \nu_{in}) - \frac{2q}{(\nu_\zeta^P - (1+2q^2)\nu_{in})} (\nu_\theta + \ell \varepsilon_0^2 \nu_{in}) \right] \quad (1)$$

where V is the volume enclosed in the flux surface, M is the ion mass, N is the plasma density, $\varepsilon_0 = r/R$ is the inverse aspect ratio, $\ell = 1/q$ is the rotational transform and $\nu_{in} = N_0 \langle \sigma v \rangle_{in}$ is the momentum loss rate due to collisions with neutrals where N_0 is the neutral density and $\langle \sigma v \rangle_{in}$ is the reaction coefficient. To obtain the above expression, a large-aspect-ratio tokamak approximation has been used for the Hamada basis vectors [9]. With the magnetic field expressed in the form $B = B_0 [1 + \sum_{mn} \varepsilon_{mn} \cos(m\theta - n\zeta)]$, where θ and ζ are the Hamada poloidal and toroidal angles, then $\nu_\theta^P = \nu_0 \alpha_P / [(1+2q^2)\varepsilon_0^2]$, $\nu_\zeta^P = \nu_0 \alpha_C / [(1+2q^2)\varepsilon_0^2]$, $\nu_\theta = \nu_0 (\alpha_P/q + \alpha_C)$, and $\nu_\zeta = \nu_0 (\alpha_C/q + \alpha_T)$. The α 's are given in the Pfirsch-Schlüter regime by $\alpha_P = 1/2 \sum_m m^2 \varepsilon_{mn}^2$, $\alpha_T = 1/2 \sum_n n^2 \varepsilon_{mn}^2$ and $\alpha_C = -1/2 \sum_{mn} mn \varepsilon_{mn}^2$ and ν_0 is a frequency defined by $\nu_0 = 2.048 v_t^2 / [(\nu_{ii} + \nu_{in}) R^2]$ where v_t is the ion thermal velocity, ν_{ii} is the ion-ion collision frequency and R is the major radius. In the plateau regime, all the above equations hold with the substitution $\varepsilon_{mn}^2 \rightarrow \varepsilon_{mn}^2 / |n - m\ell|$ and $\nu_0 = \sqrt{\pi} v_t / R$.

In the limit of vanishing viscosity, Eq. (1) yields

$$\sigma_r = \frac{c^2 MN \nu_{in} (1+2q^2)}{B_0^2} \quad (2)$$

which is in agreement with an earlier result by Yoshikawa [10]. For an axisymmetric tokamak with neutrals, the radial conductivity in the plateau regime is given by

$$\sigma_r = \frac{c^2 MN \nu_{in} (1+2q^2)}{B_0^2} \frac{\frac{\nu_0 q}{2(1+2q^2)} + \nu_{in}}{\frac{\nu_0 \varepsilon_0^2}{2q} + \nu_{in}} \quad (3)$$

The combination of viscosity and neutrals in a tokamak can increase the radial conductivity over the Yoshikawa expression by factors on the order of 2-5.

A biased electrode is used to induce a radial electric field and plasma flow on different magnetic surfaces in IMS. The potential in the plasma is measured both with an emissive probe and an array of floating probes. From the bias current, the magnetic surface area and the radial electric field, the radial electric conductivity is calculated and compared to Eq. (1) as a function of neutral pressure. Figure 1 shows a comparison of the theory and experiment for two radial locations, $R = 41.0$ cm and 42.0 cm.

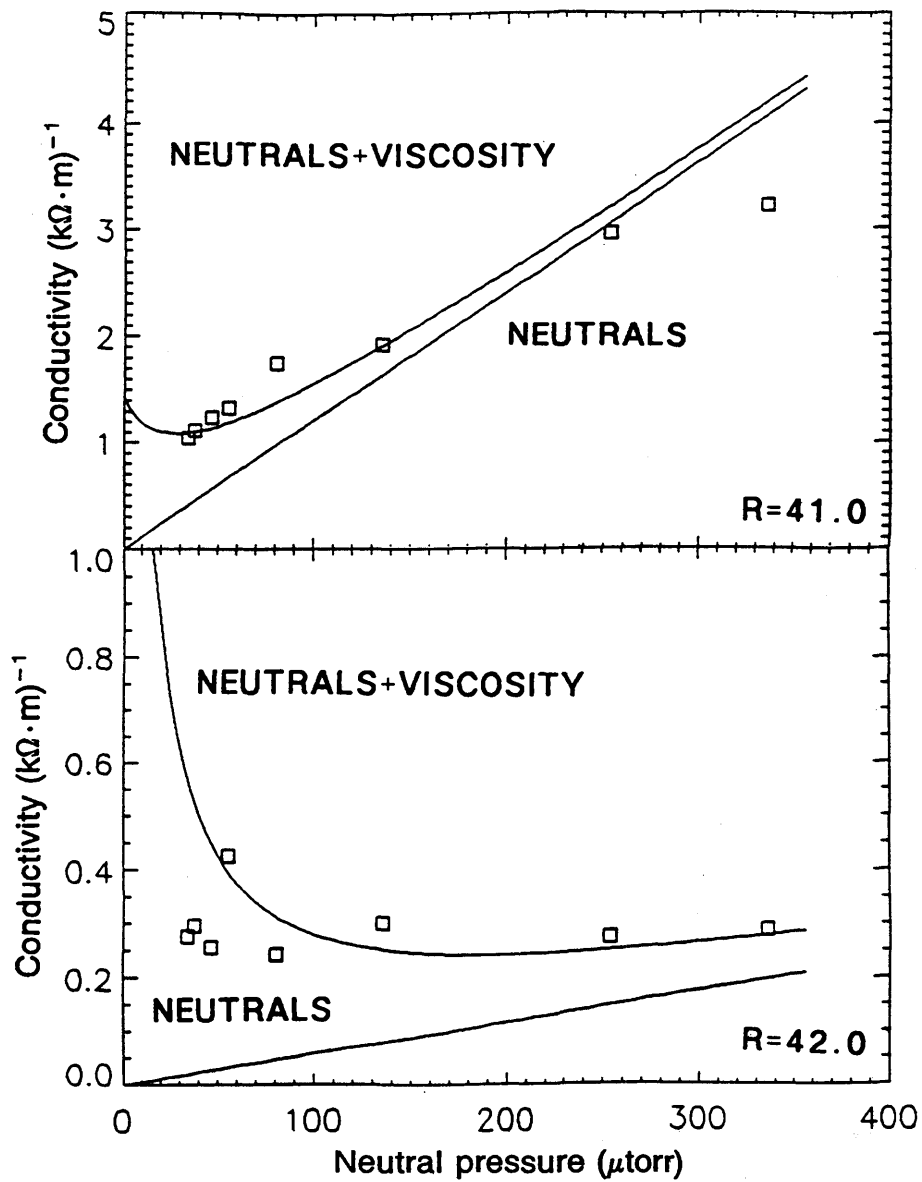


FIG. 1. Radial electric conductivity versus neutral pressure interior to the plasma at $R = 41.0$ cm (top) and near the plasma edge at $R = 42.0$ cm (bottom). Theoretical calculations that include both viscosity and collisions with neutrals, Eq. (1), and damping only due to neutrals, Eq. (3), are also shown.

The magnetic axis is located at $R = 38.1$ cm and the separatrix is at $R = 42.5$ cm. The experimental data has been normalized to the theory in the figure. When the electrode is interior to the plasma, the conductivity increases with the neutral pressure in approximately the manner predicted by the Yoshikawa expression of Eq. (2). Closer to the plasma edge where the viscosity is larger, the conductivity is roughly independent of the neutral density.

The plasma flow U is related to the radial current I by

$$U = \frac{I_c}{\sigma_r A B_0} \frac{v_\zeta + v_{in}}{I v_\theta + v_\zeta + v_{in}} \left[\theta - \left(2q \cos \theta + \frac{v_\theta + \epsilon_0^2 v_{in}/q}{\epsilon_0 (v_\zeta + v_{in})} \right) \phi \right] \quad (4)$$

where A is the magnetic surface area. In the limit of vanishing viscosity, the flow is given by

$$U = \frac{I B_0}{A c N M v_{in} (1 + 2q^2)} (\theta - 2q \cos \theta \phi) \quad (5)$$

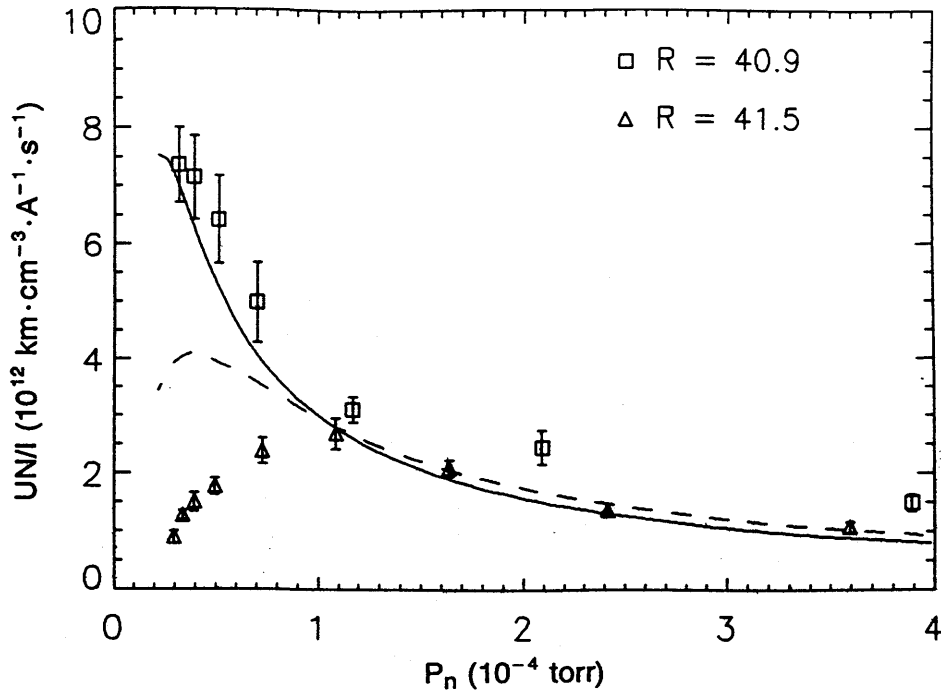


FIG. 2. Magnitude of normalized flow velocity, UN/I , versus neutral pressure at $R = 40.9$ cm and $R = 41.5$ cm. The solid and dashed curves are the theoretical calculations based on Eq. (4).

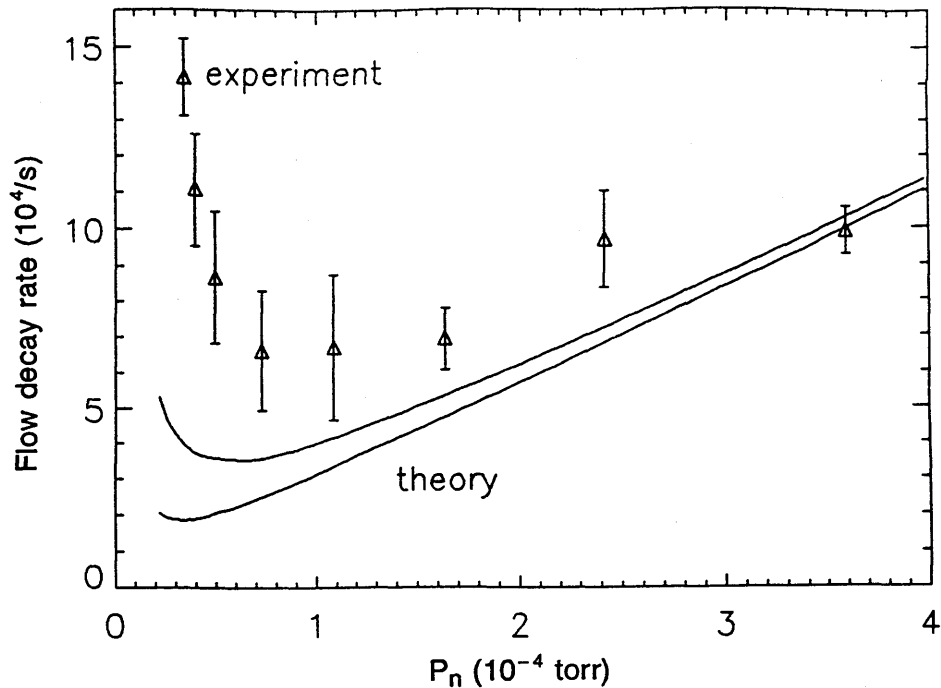


FIG. 3. Ion flow decay rate versus neutral pressure at $R = 41.5$ cm. The solid lines are the calculated minimum and maximum decay rates on the flux surface from Eq. (6).

The ion flow in IMS was measured with a Mach probe biased into ion saturation. The relationship between the ratio of the upstream to downstream current and the Mach speed can depend on whether the probe behaves in a magnetized or unmagnetized fashion [11]. The degree of magnetization of the IMS Mach probe, where the ion Larmor radius is on the order of the probe dimensions, was determined experimentally. The ion saturation signals to the upstream and downstream faces of the probe were averaged together and found to be approximately independent of the angle of the probe with respect to the magnetic field direction. Based on this observation, the theory by Hudis and Lidsky [12] for a Mach probe in an unmagnetized plasma was used to determine the plasma flow velocity. Comparison of the poloidal flow calculated using this model to the value obtained from the momentum balance equation based on measurements of the electric field and pressure gradient showed agreement to within 15%.

The total experimental flow velocity, normalized to the electrode current and plasma density, is shown in Fig. 2 versus neutral pressure for two radial locations of the biased electrode. When the Mach probe and the electrode are at the inner surface where the viscosity is small, then the flow

decreases monotonically with pressure as expected from Eq. (5). With the probe and the electrode at the outer surface, the normalized flow reaches a maximum at a neutral pressure of 1×10^{-4} Torr and then decreases as the neutral density is increased. This agrees qualitatively with the theoretical model. Small errors in the location of the probe can account for the discrepancy because of the strong variation of the viscosity as a function of radius. From Eq. (5) it can be seen that the ratio of the toroidal to poloidal flow should be approximately $2q$, because of the Pfirsch-Schlüter component to the flow. Instead the experimental data from the Mach probe indicates that the flow is mostly in the poloidal direction. The reason for this discrepancy is unknown at present; however, a comparison of the Mach probe data on either side of the magnetic axis indicates that the toroidal flow does indeed reverse sign across the magnetic axis.

The time-dependent solution to the continuity and momentum balance equations yield two characteristic damping rates on a flux surface given in Ref. [8] by

$$\begin{aligned}\omega^+ &= \nu_{in} + \nu_{visc}^+ \\ \omega^- &= \nu_{in} + \nu_{visc}^- \end{aligned} \quad (6)$$

$\nu_{visc}^\pm = \nu_1/2 \pm [(\nu_1/2)^2 + (\nu_\zeta^P \nu_\theta - \nu_\theta^P \nu_\zeta)]^{1/2}$ and $\nu_1 = \nu_\theta^P + 2q\nu_\theta/(1+2q^2) + \nu_\zeta$. In the limiting case that viscosity is negligible with respect to collisions with neutrals, the two damping times are the same and equal to ν_{in} . By disconnecting the bias on the electrode midway through the discharge, the decay in the plasma rotation could be observed with the Mach probe. The ion flow decay rate is shown in Fig. 3 as the neutral pressure is varied at a radial location where viscosity is non-negligible. Also shown are the minimum and maximum decay rates on the flux surface as predicted by the model. The data indicates that the decay rate at low pressure decreases with the neutral density, reaches a minimum and then increases again as the neutral density is further increased.

3. H-MODE THEORY IN STELLARATORS

To determine whether the radial electric field in a stellarator will undergo a bifurcation, the poloidal and toroidal flows as well as the pressure gradient need to be calculated. Because the toroidal flow (and thus the parallel flow $U_{||}$) is damped by the toroidal viscosity in stellarators, we assume $U_{||} \approx 0$ and only consider the poloidal component of the momentum equation in Hamada coordinates:

$$NM \frac{\partial}{\partial t} \langle \mathbf{B}_p \cdot \mathbf{U} \rangle = - \langle \mathbf{B}_p \cdot \nabla \cdot \boldsymbol{\pi} \rangle - \nu_{in} NM \langle \mathbf{B}_p \cdot \mathbf{U} \rangle - (\psi' \chi' / c) \langle \mathbf{J} \cdot \nabla \mathbf{V} \rangle \quad (7)$$

where the brackets denote the flux surface average, $\mathbf{B}_p = -\chi' \nabla \mathbf{V} \times \nabla \zeta$, $\psi' = \mathbf{B} \cdot \nabla \zeta$, $\chi' = \mathbf{B} \cdot \nabla \theta$, and the radial current density, $\langle \mathbf{J} \cdot \nabla \mathbf{V} \rangle = (1/4\pi) \partial \langle \mathbf{E} \cdot \nabla \mathbf{V} \rangle / \partial t$ is given by Ampère's law. For a large-aspect-ratio stellarator

with a magnetic field spectrum, $B = B_0 [1 + \sum_{mn} \epsilon_{mn} \cos(m\theta - n\zeta)]$, the poloidal viscosity is given by

$$\langle \mathbf{B}_p \cdot \nabla \cdot \boldsymbol{\pi} \rangle = \frac{\sqrt{\pi}}{4} N M v_t B \sum_{mn} [I_{mn} \epsilon_{mn}^2 m (m \mathbf{U} \cdot \nabla \theta - n \mathbf{U} \cdot \nabla \zeta) + L_{mn} \epsilon_{mn}^2 m (2/5 p) (m \mathbf{q} \cdot \nabla \theta - n \mathbf{q} \cdot \nabla \zeta)] \quad (8)$$

Here p is the plasma pressure and \mathbf{q} is the heat flow. The energy integrals I_{mn} and L_{mn} are defined as $\{I_{mn}, L_{mn}\} = (1/\pi) \int_0^\infty dx x^2 e^{-x} \{1, x - \frac{5}{2}\} \int_{-1}^1 dy (1-3y^2)^2 (v\chi'/B) R_{mn}$, where $R_{mn} = v_k / [(m\omega_\theta - n\omega_\zeta)^2 + v_k^2]$, $\omega_\theta = (v_{||} + U_{||})\chi'/B + \mathbf{V}_E \cdot \nabla \theta$, $\omega_\zeta = (v_{||} + U_{||})\psi'/B + \mathbf{V}_E \cdot \nabla \zeta$, \mathbf{V}_E is the $\mathbf{E} \times \mathbf{B}$ velocity, v is the particle speed, $v_k = 3v_D + v_E$, v_D and v_E are defined in Ref. [13].

To express Eqs. (7)-(8) in terms of the cylindrical coordinates (r, θ, ϕ) , we adopt the formula derived in Ref. [9] for tokamaks and note that our results are approximately valid. With the assumption that $q_{||} \sim 0$, we obtain:

$$-\frac{\langle \mathbf{B}_p \cdot \nabla \cdot \boldsymbol{\pi} \rangle_{\text{orbit}}}{N M v_t^2 \chi'} = \frac{\sqrt{\pi}}{4} \sum_{mn} \epsilon_{mn}^2 m (m - nq) \left\{ I_{mn} \left[\frac{U_{||}}{v_t} + \frac{m}{m - nq} (M_p - V_{p,p}) \right] - L_{mn} \frac{m}{m - nq} V_{p,T} \right\} + \epsilon_t^2 \frac{v_{in}}{(v_t/Rq)} \left(\frac{U_{||}}{v_t q^2} + \frac{1+2q^2}{q^2} (M_p - V_{p,p}) \right) \quad (9)$$

where $V_{p,p} = -c(dp/dr)/(Nev_t B_p)$ and $V_{p,T} = -c(dT/dr)/(ev_t B_p)$. In Eq. (9) we have separated the hot particle contributions to $\langle \mathbf{B}_p \cdot \nabla \cdot \boldsymbol{\pi} \rangle$ as an orbit loss term. The poloidal Mach number is defined as $M_p = -cE_r/(B_p v_t)$. For $E_r < 0$, M_p is positive.

TABLE I. MODEL MAGNETIC FIELD SPECTRUM

	ϵ_{10}	ϵ_{11}	ϵ_{-11}	ϵ_{21}	ϵ_{12}	q_{edge}
CHS (N=8)	0.136	0.0	0.0	0.21	0.0	1.25
H-E (N=19)	0.10	0.0	0.0	0.25	0.0	0.5
LHD (N=10)	0.14	0.0	0.0	0.24	0.0	1.0
W7-AS (N=5)	0.053	0.0	0.036	0.025	0.024	1.92
HSX (N=4)	0.0	0.14	0.0	0.0	0.0	0.89

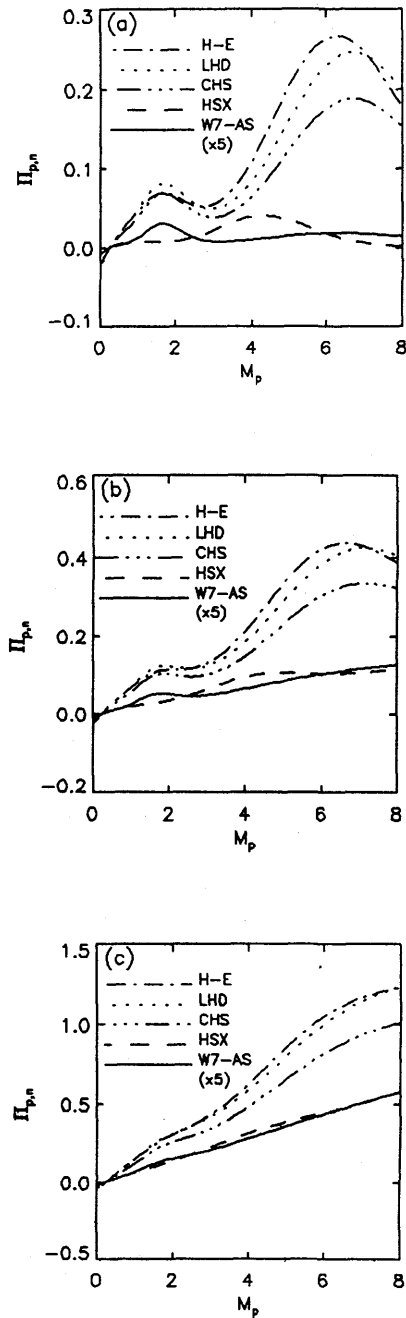


FIG. 4. Normalized plasma viscosity $\Pi_{p,n}$ versus poloidal Mach number M_p for Heliotron-E, LHD, CHS, HSX and W7-AS ($\times 5$) with $V_{p,p} = 0.2$ and $V_{p,T} = 0.1$. (a) $\nu_{*i} = 1.0$, $\nu_{in}/(\nu_i/Rq) = 0$; (b) $\nu_{*i} = 1.0$, $\nu_{in}/(\nu_i/Rq) = 0.2$; (c) $\nu_{*i} = 1.0$, $\nu_{in}/(\nu_i/Rq) = 1.0$.

With the assumption that $U_{||} \approx 0$, the right side of Eq. (9) becomes an equation for E_r for a given set of values of $V_{p,p}$ and $V_{p,T}$. In Fig. 4 we show the normalized poloidal viscosity $\pi_{p,n}$, which is the right side of Eq. (9) divided by $\sqrt{\pi}/4$, for CHS, Heliotron-E, LHD, W7-AS and HSX with $V_{p,p} = 0.2$ and $V_{p,T} = 0.1$. The values of ϵ_{mn} and q for these devices are shown in Table I. The toroidal mode number, n , listed in the table is for one field period for each experiment. In Fig. 4a, the effect of charge-exchange momentum loss is neglected and $U_{*i} = v_k R q / (v_t \epsilon_t^{3/2}) = 1$. We see that $\pi_{p,n}$ has two local maxima for CHS, Heliotron-E and LHD. The first maximum is the toroidal maximum, located at $M_p \simeq 1.7$, and the second is the helical maximum, located at $M_p \simeq 6.5$, which is about a factor of $|m-nq|/m$ higher than the first.

The physical origin of the two local maxima can be understood from the resonant term R_{mn} and particularly the resonant denominator $m\omega_\theta - n\omega_\zeta$. In a simplified form, $m\omega_\theta - n\omega_\zeta = (v\chi'/B)(m-nq)\{(v_{||}/v) + (U_{||}/v) + M_p [m/(m-nq)](v_t/v)\}$. If $U_{||}/v_t \approx 0$, for each (m,n) mode, $m\omega_\theta - n\omega_\zeta \approx 0$ when $(v_{||}/v) \sim M_p [m/(m-nq)](v_t/v)$. For the $(1,0)$ mode, resonance occurs at $M_p \simeq 1$. For the (m,n) mode, this happens at $M_p \sim |m-nq|/m$ for $E_r < 0$. The existence of multiple resonances for a stellarator was also observed numerically by Maassberg using the DKES code [14]. A stellarator usually has at least two Fourier harmonics in the magnetic field spectrum. Thus $\langle \mathbf{B}_p \cdot \nabla \cdot \boldsymbol{\pi} \rangle$ can have two local maxima. The helical maximum can disappear as in the W7-AS case due to a larger toroidal curvature component. Thus W7-AS is very similar to a tokamak. Because the toroidal maximum in W7-AS is smaller than that in other stellarators, it is easier for the radial electric field in W7-AS to bifurcate. HSX has only one maximum at $M_p \sim 4.3$ due to the helical component of the spectrum. This device is a quasi-helical toroidal stellarator with negligible toroidal curvature. It is thus different from other stellarators and tokamaks in that bifurcation should only occur at a relatively high poloidal Mach number.

To observe the local maximum of the poloidal viscosity, the charge-exchange momentum loss must be reduced by controlling the neutral density. As we increase $v_{in}/(v_t/Rq)$ from 0 to 0.2, the toroidal local maximum almost disappears as shown in Fig. 4b. If we further increase the neutral density, not only the toroidal local maximum but also the helical local maximum can be made to disappear, as shown in Fig. 4c.

Acknowledgements

This work was supported in part by the U.S. Department of Energy under grant DE-FG02-93ER54222 and under contract DE-AC05-84OR21400 with Martin Marietta Energy Systems, Inc. M.Y. would like to acknowledge JSPS Research Fellowship for Young Scientists.

References

- [1] SHAINING, K.C., CRUME, E.C., Jr., Phys. Rev. Lett. **63** (1989) 2369.
- [2] SHAINING, K.C., CRUME, E.C., Jr., HOULBERG, W.A., Phys. Fluids B **2** (1990) 1496.
- [3] ITOH, K., ITOH, S.-I., Nucl. Fusion **32** (1992) 2243.
- [4] TAYLOR, R.J., et al., Phys. Rev. Lett. **63** (1989) 2365.
- [5] WEYNANTS, R.R., in Plasma Physics and Controlled Nuclear Fusion Research 1990 (Proc. 13th Int. Conf. Washington, D.C., 1990), Vol. 1, IAEA, Vienna (1991) 473.
- [6] IDA, K., et al., Phys. Rev. Lett. **65** (1990) 1364.
- [7] GROEBNER, R.J., BURRELL, K.H., SERAYDARIAN, R.P., Phys. Rev. Lett. **64** (1990) 3015.
- [8] CORONADO, M., TALMADGE, J.N., Phys. Fluids B **5** (1993) 1200.
- [9] CORONADO, M., TREJO, J. GALINDO, Phys. Fluids B **2** (1990) 530.
- [10] YOSHIKAWA, S., Transverse Electrical Conductivity of a Toroidal Plasma, Rep. MATT-346, PPPL (1965).
- [11] CHUNG, K.-S., HUTCHINSON, I.H., LABOMBARD, B., CONN, R.W., Phys. Fluids B **1** (1989) 2229.
- [12] HUDIS, M., LIDSKY, L.M., J. Appl. Phys. **41** (1970) 5011.
- [13] HIRSHMAN, S.P., SIGMAR, D.J., Nucl. Fusion **21** (1976) 1079.
- [14] MAASSBERG, H., et al., Phys. Fluids B **5** (1993) 3627.

DISCUSSION

K. IDA: Why does the viscosity increase when the neutral pressure decreases?

J.N. TALMADGE: Damping due to parallel viscosity is caused by the ripple in the magnetic field on the flux surface. As the collisionality decreases, the drag on the fluid due to this bumpiness increases in the Pfirsch-Schlüter regime.

K. IDA: Since damping due to collisions between neutrals and ions is homogeneous, one can expect the poloidal and toroidal flows to tend towards the same magnitude as the neutral pressure is increased. Did you observe this phenomenon?

J.N. TALMADGE: Even as the damping due to neutrals increases, the toroidal and poloidal flows are not the same. This is because of the incompressibility of the fluid. As the fluid is forced to flow in the poloidal direction, a Pfirsch-Schlüter component to the toroidal flow also exists. The ratio of the toroidal to poloidal flow velocity goes like $2q\cos\theta$. We have observed that the toroidal flow reverses sign on either side of the magnetic axis, confirming the existence of the Pfirsch-Schlüter flow.